Neuroendocrinology Letters Volume 36 No. 8 2015
ISSN: 0172-780X; ISSN-L: 0172-780X; Electronic/Online ISSN: 2354-4716
Web of Knowledge / Web of Science: Neuroendocrinol Lett
Pub Med / Medline: Neuro Endocrinol Lett

The effects of the auditory brainstem response before and after fluoro-gold injection in medial geniculate body

Meichan Zhu[#], Guangyao He[#], Heng Li, Mao Xie, Bibek Gyanwali, Lihong Xie, Yikang Liu, Songhua Tan, Tiansong Lin, Anzhou Tang

Department of Otorhinolaryngology and Head and Neck Surgery, First Affiliated Hospital of Guangxi Medical University, Nanning, Guangxi, China

[#] *These authors contributed to the work equally and should be regarded as co-first authors.*

Correspondence to: Anzhou Tang, PhD.
Department of Otorhinolaryngology and Head and Neck Surgery
First Affiliated Hospital of Guangxi Medical University
No.6 Shuangyong Road, 530021 Nanning, Guangxi, China.
tel: +86-15078892243; e-mail: anzhoutang321@163.com

Submitted: 2015-03-19 Accepted: 2015-08-08 Published online: 2015-01-23

Key words: **auditory pathway; medial geniculatebody; fluoro-gold; retrograde fluorescent tracing; auditory brainstem responses; tree shrew**

Neuroendocrinol Lett 2015; **36**(8):779–786 **PMID:** 26921579 NEL360815A09

Abstract

OBJECTIVE: This study aimed to use the tree shrew as an otological model, not only to verify the location of the auditory pathway in tree shrews by fluoro-gold (FG) but also to elucidate the effects of the auditory brainstem response (ABR) before and after FG injection.

METHODS: FG was injected into the medial geniculate body (MGB) of experimental group (n=10).The normal group (n=10) was inserted the microsyringe, which was not perfused FG. Hearing was assessed by testing ABRs before and after the operation.

RESULTS: FG-labelled neurons were primarily distributed in the ipsilateral MGB, the ipsilateral and contralateral nuclei of the inferior colliculus (NIC), the superior olivary nucleus (SON), the dorsal cochlear nucleus (DCN), and the ventral cochlear nucleus (VCN). The ABR after FG injection caused a significant decrease in the wave amplitudes at 24 h that recovered by 72 h. However, the wave I–VI interpeak latencies in the right ear were shortened at 0 and 24 h post-surgery, whereas after 48 h, the interpeak latencies were prolonged.

CONCLUSIONS: The FG retrograde tracing technique accurately displays the anatomical location of the auditory pathway in the tree shrew. The change in ABR waves suggested that there was a functional abnormality in the central auditory pathway after FG injection. The auditory thalamus may have self-regulating properties.

ORIGINAL ARTICLE

INTRODUCTION

The medial geniculate body (MGB), which is an important thalamic nucleus in the auditory system, is composed of three subparts: the ventral, dorsal, and medial parts. Oliver and Hall's early anatomical studies demonstrated that the MGB of the tree shrew has eight subdivisions, which were identified on the basis of differences in Nissl-stained material. Experiments that used anterograde and retrograde axonal tracing and anterograde degeneration have demonstrated that

each subdivision has a unique pattern of connections with the midbrain(Oliver & Hall 1975; 1978).

Schmued used a new fluorescent probe referred to as Fluoro-gold (FG) as a retrograde axonal tracer for numerous neurons. FG labelling is characterised by an intensely fluorescent golden colour. Retrograde labelling of neurons has demonstrated that this tracer is largely localised within vesicle-like structures and is secondarily associated with the plasma membrane and the nucleolus(Schmued & Fallon 1986). Recently, fluorescent tracers, such as FG and Fluoro-ruby (FR)(Lu *et al.* 2001), have received increased attention. In addition to their simple colour development processes, they provide clearer results, with less background interference than images obtained using traditional immunohistochemical methods.

The physiological effects of the descending and ascending controls on the responses of the olivocochlear efferent system have been analysed in experiments that used electrical stimulation, lesions or chemical blockade of the MGB. Clinical studies of hearing outcome of central deafness patients have indicated significant hearing loss using bothmid-latency auditory evoked potentials(Vaney *et al.* 2011; Feuerecker *et al.* 2011) and auditory brainstem response (ABR) testing(Bidelman & Syed-Khaja 2014; Yamazaki *et al.* 2014). Physiological studies havedemonstrated that corticofugal projections contribute to various forms of auditory plasticity(Zhang *et al.* 2005). For example, descending pathways can alter coding and frequency in the midbrain(Bajo *et al.* 2010) .Melcher identified both the generators of the brainstem auditory evoked potential incats and specific cell populations in the MGB(Melcher & Kiang 1996) .ABRs have been used to analyse thalamic cellular properties in postnatal rat brains(Venkataraman & Bartlett 2014). However, little is known regarding whether FG injection in the MGB changes the ABR waves.

This study aimed to use the tree shrew as an otological model, not only to verify the location of the auditory pathway in tree shrews by FG but also to elucidate the effects of the ABR on thresholds, wave amplitudes, wave I latencies, and wave I–VI interpeak latencies before and after FG injection.

MATERIAL AND METHODS

Materials

Twenty healthy, clean, adult tree shrews, including males and females, aged 1.5 years that weighed 130–170 g wereprovided by Kunming Medical University, China. All animal experimentswere conducted according to protocols approved by the Institutional Animal Care and Use Committee of Guangxi Medical University in China.

Overview of the experimental design

The ABRs of bilateral hearing in the tree shrews were recorded before the operation. FG was injected into the medial geniculate body (MGB) of experimental group (n=10).The normal group (n=10) was inserted the microsyringe ,which was not perfused FG.Based on the location of the MGB, a 4% FG solution (Biotium, USA) was delivered via a micro syringe using positive iontophoretic currents. The injections were targeted to the right MGB as determined by the atlas. The ABRs of bilateral hearing in all animals were recorded at 0, 24, 48, and 72 h after the operation. The animals were subsequently anaesthetised, perfused through the heart and fixed for 1 h with phosphate-buffered saline (pH 7.4, 4 °C) that contained 4% paraformaldehyde. Tissue for serial sections was collected three days after FG injection, and the FG cell labelling was observed.

FG retrograde tracing

The tree shrews were anaesthetised using 1% pentobarbital sodium (0.4 mL/100 g) via an intraperitoneal injection and subsequently placed in a prone position. The limbs and the heads were fixed on an locator (RWD Life Science, Shenzhen, China) prior to disinfection and skinpreparation. A 4% FG solution (Biotium, USA) was delivered in small volumes (0.05–0.25 μL) via a micro syringe and positive iontophoretic currents (5 mA/20 min, 4% dye in lactated Ringer's solution). The injections were targeted to the MGB as determined by the atlas (Figure 1-A).

The stereotaxic method was based on a three-dimensional coordinate system with three planes located at right angles to each other. The APO, or interaural plane, is a vertical plane that passes through the interaural line and divides the brain into rostral and caudal areas. Finally, the HO, or horizontal plane, is a modified zero plane that runs parallel to the axis of the brain and 4 mm above the interaural line. The plates of the horizontal sections above the HO plane are expressed in plus-millimetres, and the plates below the HO plane are expressed in minus-millimetres. The position of the MGB in the tree shrews was APO 1.8 mm, HO 1 mm, and 4 mm on the right side near the centre line (Wenguang 1990).

Tissue was collected for serial sections three days after FG injection. The animals were anaesthetised, perfusedthrough the heart and subsequently fixed for 1 h with phosphate-buffered saline (pH 7.4, 4 °C) that contained 4%paraformaldehyde. The brainand the spinal cord were removed, fixed for 24 h,and placed in successive 20% and 30% sucrosesolutions. After the tissues sank, the brain was frozen and sectioned longitudinally in serial sections of 20 μm. Two tree shrews were stained with toluidine blue, and eight tree shrews were processed for FG cell labelling.

Auditory pathway image acquisition

The sections were maintained in the dark, dried at roomtemperature, mounted with 20% glycerol, and observedunder a BX53 upright fluorescence microscope (Olympus, Japan) using wide-band ultraviolet

excitation (emission max: 418 nm, excitation max: 331 nm). Photographs were taken via 4×, 10×, and 20× objectives using Olympus DP2-BSW software (Olympus, Tokyo, Japan).

Hearing assessment

The hearing of each animal was assessed via the ABR (Tucker-Davis Technologies, TDT Company, USA) before and after the operation. Sound was delivered using a closed system, with probes carefully nestled in the ear canal. The ABRs were recorded using clicks of 0.1 ms in duration and a presentation rate of 21.0 per second. One thousand twenty-four repetitions were collected over a time window of 10 ms and averaged. The final signal was filtered with a 500-Hz high-pass filter and a 3000-Hz low-pass filter. Tests were performed using a 4-kHz click (Liao *et al.* 2013). The threshold, defined as the minimum intensity at which a specific frequency could be processed, was manually obtained for both ears. The positive and negative peaks of each wave and the latency values at 80 dB SPL were assessed. The absolute wave I latency was defined as the time in ms from the onset to the positive peak of the wave. The interpeak latencies were defined as the time in ms between the positive peaks of the different ABR waves.

Data analysis

The ABR thresholds and wave latencies obtained for each group are reported as the means. The differences between the groups were analysed by analysis of variance (ANOVA). The *p*-values of 0.05 or less were considered significant. All statistical analyses were performed with the Statistical Package for the Social Sciences (SPSS 19, Chicago, IL, USA).

RESULTS

Quantitative analysis of experimental animals

Twenty healthy, adult tree shrews wereinitially included in the experiment and the final analysis.

Visualisation of the auditory pathway of the tree shrew using FG retrograde fluorescent tracing

The left MGB and the ipsilateral nucleus of the inferior colliculus (NIC), the superior olivary nucleus (SON), the dorsal cochlear nucleus (DCN), and the ventral cochlear nucleus (VCN) of the tree shrews all exhibited FG-positive axons, which were clearlylabelled with a fluorescent gold signal that exhibited distinct boundariesbetween the labelled areas and the surrounding structures (Figure 1-B). The locations of the FG-labelled cells were consistent with the map in the tree shrew brain atlas (Figure 1-A).

The FG-labelled neurons, which were observed using a fluorescence microscope, were primarily distributed in areas of the NIC, the SON, the DCN, and the VCN (Figure 1-C).

ABR data before and after surgery

Threshold

The ABR threshold of the right FG in the injected ablated animals before surgery was 24.00±3.16 dB SPL. After surgery, the ABR threshold of the animals was 24.70±2.41 dB SPL at 0 h, 25.30±3.40 dB SPL at 24 h, 25.80±3.39 dB SPL at 48 h, and 25.70±2.98 dB SPL at 72 h. No significant differences were identified in the ABR threshold before or after surgery in the experimental and normal group.

Wave amplitudes

No significant differences were identified in the ABR amplitudes before or after surgery in the normal group. In FG group,the amplitudes of all ABR waves (II, III, IV, and VI) after stimulation of the right ear exhibited significant decreases at 24 h after the surgery compared with the values before the surgery (Figure 2-C). The decreases in the amplitudes of waves I ($p>0.05$) and V ($p>0.05$) in this experimental condition were not significant in relation to the pre-operative condition (Figure 2-D). This experimental condition exhibited significant decreases in wave III at 48 h ($p<0.01$) and wave IV at 0 h ($p<0.01$).

The ABRs from the stimulation of the left ear exhibited wave amplitudes after FG injection that were comparable with the pre-injection condition, and no significant changes were identified (Figure 2-D).

Wave latencies

No significant differences were identified in the ABR latencies before or after surgery in the normal group.

In FG group,the latencies of wave I at 24 h after the right ear was stimulated were prolonged compared with before the operation. This experimental condition exhibited a significant increase in the absolute latency of wave I ($p<0.01$). The latencies of wave I at 48 h reverted to baseline. No significant changes were identified after the stimulation of the left ear ($F=2.689$, $p=0.032$) (Figure 2, Table 1).

However, the wave I–VI interpeak latencies in the right ear were shortened at 0 and 24 h post-surgery, whereas at 48 and 72 h, the interpeak latencies were prolonged. There was a significant shortening in the wave I–VI interpeak latencies in both ears ($p<0.05$). In the left ear, the wave I–VI interpeak latencies were also shortened immediately after the surgery and became prolonged only after 24 h (Figure 2, Table 1)

DISCUSSION

A number of studies have investigated the auditory pathway in animal models (Horie *et al.* 2013; Miller & Covey 2011; Winer *et al.* 2002; Bartlett *et al.* 2011). Tree shrews have frequently been used in other fields of research (Cao *et al.* 2003; Coolen *et al.* 2012), as well as in studies of the auditory pathway. Tree shrews (Fan *et al.* 2013; Xu *et al.* 2012) are squirrel-like mammals

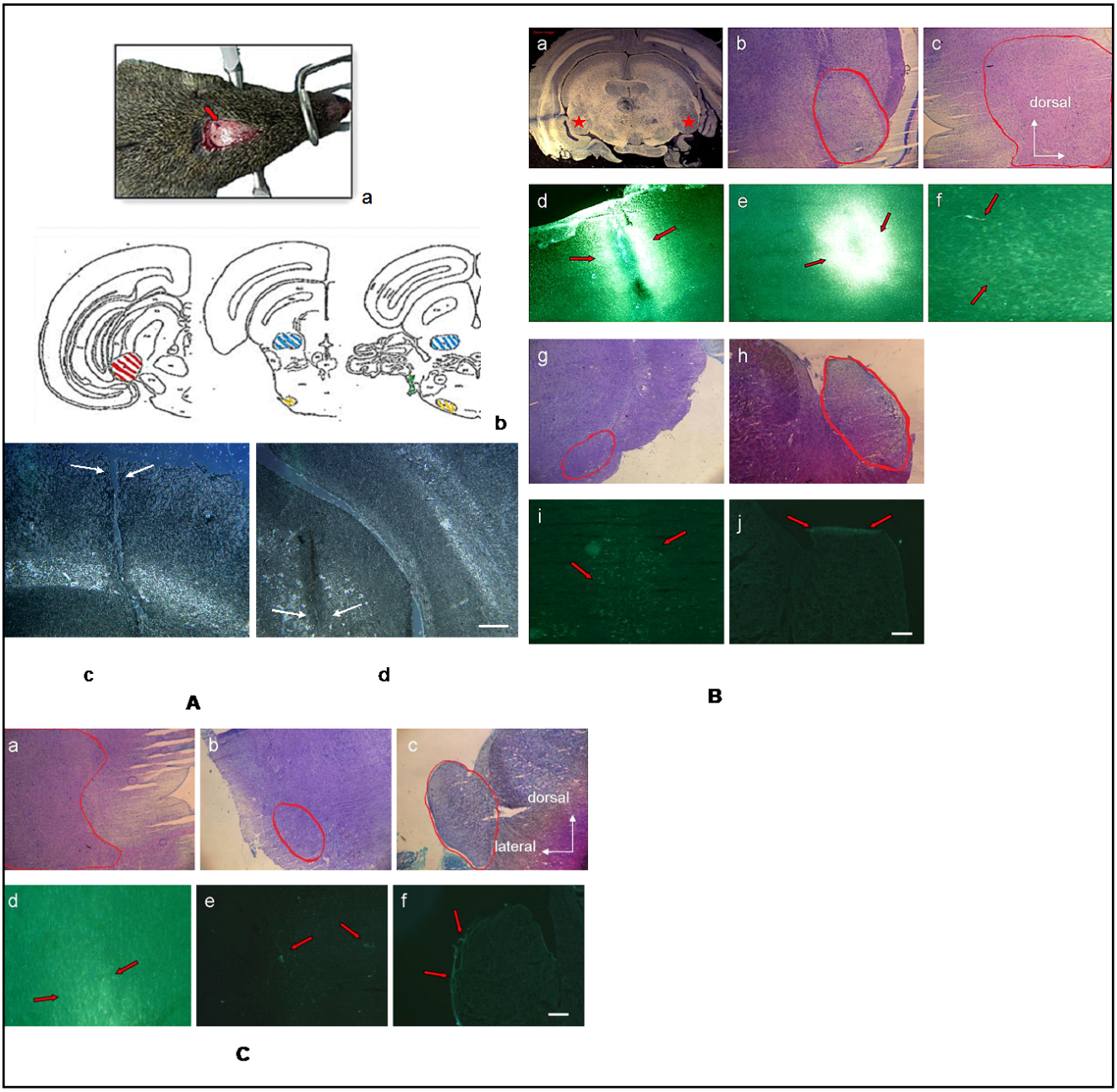

Fig. 1. A a. Location of the FG injection. **b.** Atlas of the tree shrew brain (red for the medial geniculate body (MGB), blue for the nucleus of the inferior colliculus (NIC), yellow for the superior olivary nucleus (SON), green for the dorsal cochlear nucleus (DCN) and the ventral cochlear nucleus (VCN)). **c.** Injection from the cortex, shown without staining (×40). **d.** Injection in the MGB, shown without staining (×40); scale bar=0.5 mm. **B a.** The first image in row one shows a frozen section from a tree shrew brain; the red stars indicate the MGB. **b.** Toluidine blue staining in the right MGB (×40). **c.** The NIC (×40). **d.** The injection site in the cortex (×40). **e.** FG cells (×40) visible in the right MGB. Images show three distinct zones. The first zone is centrally localised (1) and includes the needle track and a small region of necrosis. Peripheral to the first zone (2) is the bright region in which both neuropil and cells fluoresce, whereas myelinated fascicles exhibit little tracer. This middle region is presumably the zone of active terminal uptake. The most peripheral zone (3) exhibits weak cellular labelling. **f.** FG cells (×40) visible in the right NIC. **g.** Toluidine blue staining in the right SON (×40). **h.** Toluidine blue staining in the right DCN and the VCN (×40). **i.** FG cells (×40) visible in the rightSON. **j.** FG cells (×40) visible in the right DCN and VCN; scale bar=0.5 mm. **C a.** Toluidine blue staining in the left NIC (×40). **b.** Toluidine blue staining in the left SON (×40). **c.** Toluidine blue staining in the left DCN and the VCN (×40). **d.** FG cells mark the left NIC (×40). **e.** FG cells mark the left SON (×40). **f.** FG cells mark the left DCN and the VCN (×40); scale bar=0.5 mm.

and are commonly classified in the order Scandentia, between Insectivora and Primates (Muller *et al.* 1999). It has been proposed that tree shrews may represent better model animals than rodents (Baldwin *et al.* 2013) because of their closer relationship to primates.

Descending projections from the MGB to the DCN and the VCN are critical for auditory plasticity (Saldana *et al.* 1996), including the ability of central neurons to adjust their frequency tuning to relevant and meaningful stimuli (Willott 1996).

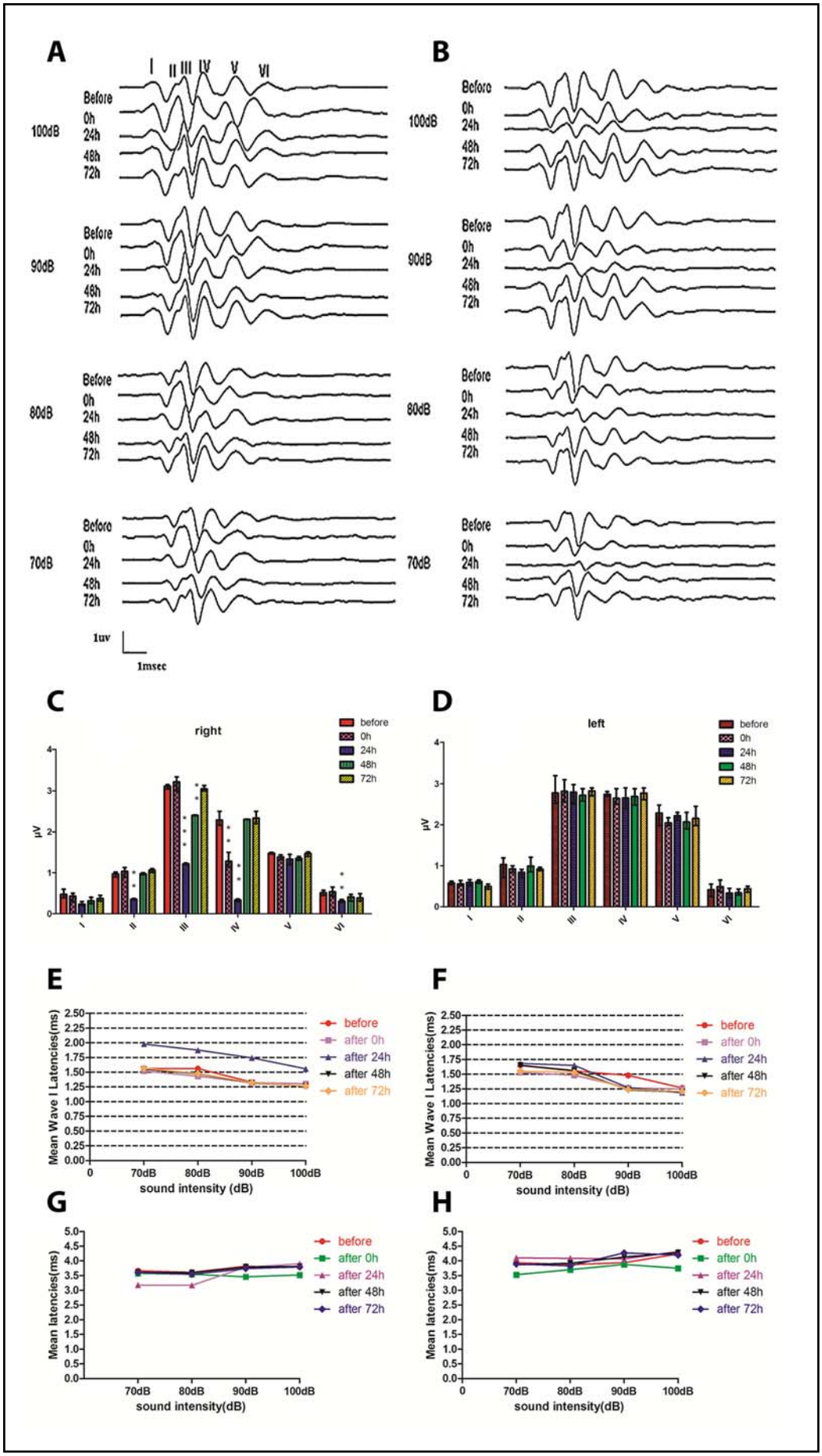

Fig. 2. A. and **B.** ABR in the left ear **(A)** and right ear **(B)** before and after FG retrograde tracing of the auditory pathway. Measurement parameters: click, 70-100 dB SPL. **C.** and **D.** ABR changes in the wave amplitudes before **(C)** and after **(D)** surgery. The graphs show the mean±SEM of the wave amplitudes in microvolts (mV). * $p<0.05$. ** $p<0.01$. *** $p<0.001$. Note that at 24 h, the wave values decrease for right ear stimulation, but no significant changes were identified for left ear stimulation. **E.** Mean wave I latencies in the right ear before and after the operation. **F.** Mean wave I latencies in the left ear before and after the operation. **G.** Mean wave I-VI interpeak latencies in the right ear before and after the operation. **H.** Mean wave I-VI interpeak latencies in the left ear before and after the operation.

Tab. 1. Auditory brainstem response latency data from different periods in Wave I and Wave I–VI.

	Right (mean (SE))	Left (mean (SE))	Right (mean (SE))	Left (mean (SE))
	Wave I latencies (ms) Groups (case number)*		Wave I–VI interpeak latencies (ms)	
1	1.43 (0.14)	1.49 (0.14)	3.72 (0.09)	4.00 (0.15)
2	1.40 (0.09)	1.38 (0.13)	3.53 (0.05)	3.72 (0.13)
3	1.79 (0.16)	1.45 (0.22)	3.51 (0.35)	4.15 (0.11)
4	1.40 (0.12)	1.41 (0.20)	3.71 (0.10)	4.05 (0.17)
5	1.41 (0.12)	1.38 (0.16)	3.67 (0.11)	4.05 (0.20)
F value (*p*-value)**	93.004 (<0.01)	2.689 (0.032)	3.901 (<0.01)	13.302 (<0.01)
p-value(1):(2)***	>0.01	—	<0.01	<0.01
p-value(1):(3)***	<0.01	—	<0.01	0.05>*p*>0.01
p-value(1):(4)***	<0.01	—	>0.01	>0.01
p-value(1):(5)***	>0.01	—	>0.01	>0.01
p-value(2):(3)***	<0.01	—	>0.01	<0.01
p-value(2):(4)***	<0.01	—	0.05 >*p*>0.01	<0.01
p-value(2):(5)***	>0.01	—	0.05 >*p*>0.01	<0.01
p-value(3):(4)***	>0.01	—	<0.01	>0.01
p-value(3):(5)***	<0.01	—	0.05 >*p*>0.01	>0.01
p-value(4):(5)***	<0.01	—	>0.01	>0.01

*group 1 = before the operation, group 2 = 0 h after the operation, group 3 = 24 h after the operation, group 4 = 48 h after the operation, group 5 = 72 h after the operation. ** indicates analysis by one-way analysis of variance; ***indicates analysis by the least significant difference test.

In this study, we utilised tree shrews as an *in vivo* model of the auditory pathway and examined the physiological effects of FG injection. Compared with nerve tracers such as biotinylated dextran amine(Veenman *et al.* 1992) and horseradish peroxidase(Karnovsky 1967), retrograde tracing with FG does not require complex immunohistochemistry or close observation during the colour reaction process. The positive staining of auditory pathway fibres on the injected side of tree shrews is visible as a clearly demarcated gold fluorescence signal, which is located in the MGB on one side of the brain and in the NIC, SON, DCN, and VCN on both sides of the brain. No FG-positive signal is observed on the contralateral side of the MGB (Figure 1-B, C). Most anatomists wait at least 7 days for FG transport. A range of 7–14 days is commonly used to allow full labelling of distal structures. We processed the tissue after 3 days because the tree shrew auditory projection is more complicated than the projection in rodents and FG transmission is fast and active(Wong *et al.* 2013) .

Longitudinal sections of the auditory pathway exhibit FG-positive labelling in cells that project from the MGB to the NIC, SON, DCN, and VCN. No positive staining is observed in the lateral MGB. Although Figure 1-C does show labelling in the SON, DCN, and VCN, this labelling is sparse. The descending projection of the MGB primarily projects to the ipsilateral nuclei rather than the contralateral nuclei. In a future study, we will determine the specific nucleus that sends the largest projection to the MGB by counting axons within each location on both the ipsilateral and contralateral sides.

Tree shrews exhibit waves I–VI in ABR checks, and they occasionally exhibit wave VII. Data from tree shrew ABR tests contain indicators similar to humans. Tree shrews consistently display wave VI of the ABR, and this response may originate from the MGB.

The changes in ABRs identified in the present study depended on the side of the FG injection and the time post-surgery of the ABR recordings. The ABR results in this study demonstrate that the tree shrews had no changes in the ABR thresholds before or after surgery. Therefore, FG injection into the MGB did not induce hearing loss.

This finding suggests that the decrease in the wave amplitude at 24 h, which recovered by 72 h, may be a consequence of the decrease in the activity of the organ of Corti and the auditory nerve following the removal of cortical inputs after FG injection by microcurrent. A future study will analyse the specific sources that affect the auditory pathway.

The wave I latencies in the left ear were the same before and after the operation. We subsequently examined the wave latencies in the right ear. The wave I–VI

interpeak latencies in the right ear were shortened at 0 and 24 h post-operation and became prolonged after 48 h. In the left ear, the wave I–VI interpeak latencies were also shortened immediately after the operation but became prolonged after only 24 h. Only at 24 h was there a difference in the ABR intensity. Taken together, these data demonstrate that the injection of FG and the microcurrent may affect the central auditory pathway. The FG and the microcurrent may have induced an acute inflammatory response at 24 h; however, the injury was minor, and recovery was observed by 48 h. The reduction in the latency time could be explained by the theory of cochlear filtering, which states that wider frequency tuning produces shorter responses. A shortening of the response leads to faster activation of nerve responses and consequently, shorter latencies of ABR waves. Eventually, afferent neurons may fire earlier if the cochlear filtering is reduced by medial olivocochlear (MOC) or lateral olivocochlear (OHC) changes(Guinan 2010). Interestingly, the present study also demonstrates that the wave amplitudes and latencies were restored by 72 h after surgery. This finding suggests a more complicated mechanism of recovery of electrical activity in the superior olivary complex, which most likely reflects a direct effect of the loss of excitation that results from injury of the descending corticofugal terminals. Additional studies will be required to determine whether FG harms the auditory pathway and to identify the mechanisms that underlie a potential effect.

We studied the morphology and electrophysiology of the tree shrew auditory pathway and successfully constructed a model of the auditory pathway using FG tracing of the neural tracts and ABR testing. However, there are difficulties associated with methods based on serial tissue sections, such as the complexity of section preparation and the long experimental procedures. Furthermore, fixed tissue is static and cannot provide insights into physiological dynamics. If *in vivo* biological tissues can be reconstructed using a combination of neural tracing and imaging methods, future research on the auditory pathway will be more effective.

The ABR changes identified in postoperative animals suggest that mechanisms in the central auditory pathway may also be involved. Nevertheless, this study provides both morphological and electrophysiological evidence that the auditory pathway of the tree shrew has otological advantages that will facilitate the transition from experimental to clinical research.

REFERENCES

1 Bajo VM, Nodal FR, Moore DR, King AJ (2010). The descending corticocollicular pathway mediates learning-induced auditory plasticity. Nat Neurosci. **13**(2): 253–260.
2 Baldwin MKL, Wei H, Reed JL, Bickford ME, Petry HM, Kaas JH (2013). Cortical projections to the superior colliculus in tree shrews (Tupaia belangeri). J Comp Neurol. **521**: 1614–1632.
3 Bartlett EL, Sadagopan S, Wang X (2011). Fine frequency tuning in monkey auditory cortex and thalamus. J Neurophysiol. **106**: 849–859.
4 Bidelman GM, Syed-Khaja A (2014). Spectrotemporal resolution tradeoff in auditory processing as revealed by human auditory brainstem responses and psychophysical indices. Neurosci Lett. **572**: 53–7.
5 Cao J, Yang EB, Su JJ, Li Y, Chow P (2003). The tree shrews: adjuncts and alternatives to primates as models for biomedical research. J Med Primatol. **32**: 123–130.
6 Coolen A, Hoffmann K, Barf RP, Fuchs E, Meerlo P (2012). Telemetric study of sleep architecture and sleep homeostasis in the day-active tree shrew Tupaia belangeri. Sleep. **35**: 879–888.
7 Fan Y, Huang ZY, Cao CC, Chen CS, Chen YX, Fan DD, He J, Hou HL, *et al.* (2013). Genome of the Chinese tree shrew. Nat Commun. **4**: 1426.
8 Feuerecker M, Lenk M, Flake G, Edelmann-Gahr V, Wiepcke D, Hornuss C, Daunderer M, Muller HH, *et al.* (2011). Effects of increasing sevoflurane MAC levels on mid-latency auditory evoked potentials in infants, schoolchildren, and the elderly. Br J Anaesth. **107**: 726–734.
9 Guinan JJ, Jr. (2010). Cochlear efferent innervation and function. Curr Opin Otolaryngol Head Neck Surg. **18**: 447–453.
10 Horie M, Tsukano H, Hishida R, Takebayashi H, Shibuki K (2013). Dual compartments of the ventral division of the medial geniculate body projecting to the core region of the auditory cortex in C57BL/6 mice. Neurosci Res. **76**: 207–212.
11 Karnovsky MJ (1967). The ultrastructural basis of capillary permeability studied with peroxidase as a tracer. J Cell Biol. **35**: 213–236.
12 Liao T, Tang A, Sun K, Xie L, Zhu K, Xie M (2013). Research of auditory brainstem response of tree shrews in China. Chin J Clin Rational Drug Use(Chinese). **6**: 93–94.
13 Lu J, Ashwell KW, Hayek R, Waite P (2001). Fluororuby as a marker for detection of acute axonal injury in rat spinal cord. Brain Res. **915**: 118–123.
14 Melcher JR, Kiang NY (1996). Generators of the brainstem auditory evoked potential in cat. III: Identified cell populations. Hear Res. **93**: 52–71.
15 Miller K, Covey E (2011). Comparison of auditory responses in the medial geniculate and pontine gray of the big brown bat, Eptesicus fuscus. Hear Res. **275**: 53–65.
16 Muller S, Stanyon R, O'brien PC, Ferguson-Smith MA, Plesker R, Wienberg J (1999). Defining the ancestral karyotype of all primates by multidirectional chromosome painting between tree shrews, lemurs and humans. Chromosoma. **108**: 393–400.
17 Oliver DL, Hall WC (1975). Subdivisions of the medial geniculate body in the tree shrew (Tupaia glis). Brain Res. **86**: 217–227.
18 Oliver DL, Hall WC (1978). The medial geniculate body of the tree shrew, Tupaia glis. I. Cytoarchitecture and midbrain connections. J Comp Neurol. **182**: 423–458.
19 Saldana E, Feliciano M, Mugnaini E (1996). Distribution of descending projections from primary auditory neocortex to inferior colliculus mimics the topography of intracollicular projections. J Comp Neurol. **371**: 15–40.
20 Schmued LC, Fallon JH (1986). Fluoro-Gold: a new fluorescent retrograde axonal tracer with numerous unique properties. Brain Res. **377**: 147–154.
21 Vaney N, Anjana Y, Khaliq F (2011). No auditory conduction abnormality in children with attention deficit hyperactivity disorder. Functional Neurol. **26**: 159–163.
22 Veenman CL, Reiner A, Honig MG (1992). Biotinylated dextran amine as an anterograde tracer for single- and double-labeling studies. J Neurosci Methods. **41**: 239–254.
23 Venkataraman Y, Bartlett EL (2014). Postnatal development of auditory central evoked responses and thalamic cellular properties. Dev Neurobiol. **74**: 541–555.
24 Wenguang Y (1990). A Stereotaxic Atlas of the Brain of Tupaia Belangeri and Macaque Monkey Living in Guangxi Guangxi, China: Guangxi Science and Technology Publishing House.
25 Willott JF (1996). Physiological plasticity in the auditory system and its possible relevance to hearing aid use, deprivation effects, and acclimatization. Ear Hear. **17**: 66S–77S.

26 Winer JA, Chernock ML, Larue DT, Cheung SW (2002). Descending projections to the inferior colliculus from the posterior thalamus and the auditory cortex in rat, cat, and monkey. Hear Res. **168**: 181–195.
27 Wong P, Peebles JK, Asplund CL, Collins CE, Herculano-Houzel S, Kaas JH (2013). Faster scaling of auditory neurons in cortical areas relative to subcortical structures in primate brains. Brain Behav Evol. **81**: 209–218.
28 Xu L, Chen SY, Nie WH, Jiang XL, Yao YG (2012). Evaluating the phylogenetic position of Chinese tree shrew (Tupaia belangeri chinensis) based on complete mitochondrial genome: implication for using tree shrew as an alternative experimental animal to primates in biomedical research. Journal of genetics and genomics = Yi chuan xue bao. **39**: 131–137.
29 Yamazaki H, Naito Y, Fujiwara K, Moroto S, Yamamoto R, Yamazaki T, Sasaki I (2014). Electrically evoked auditory brainstem response-based evaluation of the spatial distribution of auditory neuronal tissue in common cavity deformities. Otol Neurotol. **35**(8): 1394–402.
30 Zhang Y, Hakes JJ, Bonfield SP, Yan J (2005). Corticofugal feedback for auditory midbrain plasticity elicited by tones and electrical stimulation of basal forebrain in mice. Eur J Neurosci. **22**: 871–879.